Journal of Materials and Engineering Structures

Research Paper

Random Dense Packing Parameters of Two-Dimensional Spherical Powders for Hot Isostatic Pressing Process Modeling

Locif REDOUANI [a] *, Sarra KHILOUF [a], Rebah LAIDI [a], Said ALEM [b]

[a] *Laboratory of Physicochemistry of Materials, Faculty of Sciences and Technology, Chadli Bendjedid – El Tarf University, 36000, El Tarf, Algeria*

[b] *Solid Mechanics and Systems Laboratory, Faculty of Technology, University M'Hamed Bougara Boumerdes, 35000, Boumerdes, Algeria*

ARTICLE INFO

ABSTRACT

In this paper, we have used the hot isostatic pressing HIP models previously carried out for the study of the random dense packing densification (RDP) of spherical particles of the same size in order to adapt them to the RDP of two-dimensional spherical particles. A new microscopic approach is thus developed that allows the densification parameters of two-dimensional spherical powder aggregates to be evaluated as a function of the relative density, taking into account the morphological changes of the powder particles and the porosity. The equations obtained for each parameter (coordination number, mean contact area and effective pressure) made it possible to represent the results in the form of curves. These show that our new approach is well adapted to a realistic description of the densification of powder aggregates with particles of more or less similar sizes.

1 Introduction

The micromechanical modelling of hot isostatic pressing (HIP) consists in estimating the contributions of the various elementary mechanisms that can occur during the densification process. Thus, to simplify the study of the powder aggregates densification, we assimilate them to Random Dense Packing (RDP) of spherical particles. For several years, a significant effort has been devoted to HIP modelling [1-10] where RDP particles are considered spherical and one-dimensional.

RESEARCH REVIEW of
Sciences and Technologies

We speak of RDP when the powder is poured into a container that is vibrated until the compaction is stable. The relative density (D) of the latter is close to 64% (relative porosity of 36%), similar to the packing density. This packing is as compact as possible, obtained without remote control or deformation [11, 12].

This simplifies considerably the study of densification mechanisms. However, several experimental studies [1, 2, 13, 14] have revealed that the powder grain size distribution leads to significant discrepancies between experimental data and simulation results [4, 9]. On the other hand, taking into account all the sizes of the packing particles in the calculations is very difficult. Thus, recent researches, concerning mainly the coordination study [15, 16], assume that it is more convenient to consider RDPs of spheres with two different radii.

In this paper, although we refer to our previous work [6-8], the objective is different. This involves considering two-dimensional spheres in the study of RDP parameters. So, new equations will be developed to study the evolution of the coordination number (Z), the contact area (a) and the effective pressure (P_{eff}) as a function of the relative density. The morphological changes of powder aggregates during densification will also be taken into account. The results can be used for the calculation of HIP densification mechanisms equations.

2 RDP parameters

Evaluating the RDPs parameters is an essential step in HIP modeling. It takes into account the morphological changes in the porosity within the tablet during the densification process. Indeed, studies take into account two stages [4]:

- Stage I, where D is between 0.64 and 0.92. In this case, the porosity is open and interconnected.

- Stage II, with D which evolves from 0.92 to 1, characterized by an isolated porosity and of spherical shape.

- Thus, Z, a, and Peff, are evaluated as a function of D by considering these two stages.

2.1 Coordination number

Models of Artz [11] and Helle [2] assumed that Z increases during the densification of an RDP, of the same dimension spherical particles, until reaching a value of 14 at the end of densification.

In a previous work [4], we have shown that Z can't in any case exceed 12 and, moreover, it is constant in stage II since the porosity is closed. Therefore, for particles of different radii (R1 and R2), we estimate that Z can reach 14 at the end of stage I (D=0.92). Then it remains constant until complete densification.

On the other hand, we estimate that Z evolves in two steps at stage I of densification. When D is near its initial value (0.64≤D≤0.75), we admit that the expression of the coordination number can be obtained from the 1st order Taylor expansion of the expression giving the radius of particles as function of D (Eq. 1) combined with the cumulative radial distribution (Eq. 2) [5, 11].

$$R' = R \left(\frac{D}{D_0}\right)^{1/3} \tag{1}$$

with Do (Do=0.64) the initial relative density of the RDP.

$$\begin{cases} G(r) = 0 & \text{if } r < 2R \\ G(r) = Z_0 + C\left(\frac{r}{2R} - 1\right) & \text{if } r \geq 2R \end{cases} \tag{2}$$

where Z_0 (Z_0=7.3) is the initial coordination number and C (C=15.5) is the G(r) function slope.

Thus, the following equation is obtained:

$$Z = Z_0 + \frac{1}{3} C \left(\frac{D - D_0}{D_0}\right) \tag{3}$$

After replacing C and Do by their values, Z in the 1st step of stage I can be computed by the following equation:

$$Z = Z_0 + 8{,}07(D - 0.64) \tag{4}$$

The 2nd step of stage I corresponds to D between 0.75 and 0.92 where Z evolves rapidly until reaching the maximum value 14. Adding a 3rd order term at the equation (4), the relation that describes Z in the 2nd step of stage I is as follows:

$$Z = Z_0 + c_1 + 8.07(D - 0.75) + c_2(D - 0.75)^3 \tag{5}$$

where c1 and c2 are constants which ensure the continuity of the function Z(D) between the two steps of stage I.

Taking into account the boundary conditions, the equation (5) can be written as:

$$Z = Z_0 + 0.89 + 8.07(D - 0.75) + 903(D - 0.75)^3 \tag{6}$$

Therefore, and in summary, the coordination number throughout the densification process can be computed by the following equation:

$$\begin{cases} Z = Z_0 + 8{,}07(D - 0.64) & 0.64 \le D \le 0.75 \\ Z = Z_0 + 0.89 + 8.07(D - 0.75) + 903(D - 0.75)^3 & 0.75 < D \le 0.92 \\ Z = 14 & 0.92 < D \le 1 \end{cases} \tag{7}$$

2.2 Average contact area

We sought to develop new equations to evaluate the average contact area between the two-dimensional particles of an RDP.

In stage I, the densification process is modeled by the particle's growth [4, 11], (i.e. each spherical particle increases its radius around its fixed center). Thus, initial radii of the two particles are R1 and R2; their new radii are respectively R′1 and R′2 that is illustrated in Fig. 1.
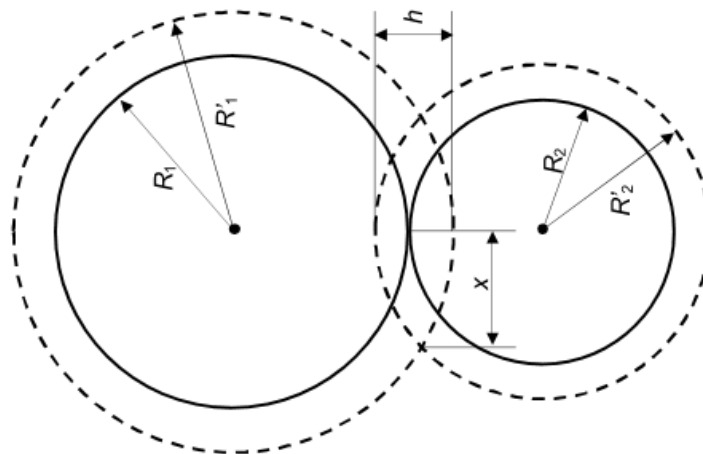

Fig. 1 – Growth and overlapping of two spherical particles of different radii (x: radius of the circular contact, h: overlapping distance).

Taking again the equation of the particle radius (Eq.1) and using the radii of the two spheres, we access to the expression giving the new radii of the particles according to the initial radii and the relative density, which is as follows:

$$\begin{cases} R'_1 = R_1 \left(\dfrac{D}{D_0}\right)^{1/3} \\ R'_2 = R_2 \left(\dfrac{D}{D_0}\right)^{1/3} \end{cases} \tag{8}$$

Geometric considerations make it possible to approach the overlapping distance by:

$$h = (R_1' - R_1) + (R_2' - R_2) \tag{9}$$

Hertz investigations [17, 18] on the elastic contacts between spherical particles are shown that the overlapping distance between two spherical one-dimensional particles can be written as follows [4]:

$$h = 2\frac{x^2}{R} \tag{10}$$

Meanwhile, Olmos Navarette [13] defined an equivalent radius (R), proposed by Pan and used by Martin [19], for each pair of particles in contact, and given by:

$$R = 2\left(\frac{R_1 R_2}{R_1 + R_2}\right) \tag{11}$$

Knowing that a=πx2 and combining this with the relations of h and R, we find:

$$a = \pi\left[\left(R_1' - R_1\right) + \left(R_2' - R_2\right)\right]\frac{R_1 R_2}{R_1 + R_2} \tag{12}$$

Replacing R′1 and R′2 by their expressions (Eq. 8) in the equation (12) and after simplification, we obtain the equation of the average contact area at the stage I defined by:

$$a = \pi R_1 R_2 \left[\left(\frac{D}{D_0}\right)^{1/3} - 1\right] \tag{13}$$

In the final stage of densification, the pores are isolated and spherical in shape. As the contacts number is equal to 14, we adopt the Ashby model to describe the shape of the particles in this stage. Indeed, Ashby and his collaborators [1, 2, 20] assimilate the powder particles to Tetradecahedra (Kelvin polyhedron), where the 24 apexes are occupied by the residual spherical pores and its 14 facets correspond to the contact areas as illustrated by Fig. 2.

However, it should be noted that Ashby used this model for particles of the same size. Whereas in our case, we adopt it for particles of two different sizes. Indeed, we observe in Fig. 2 that the polyhedron has two types of facets. The first corresponds to regular hexagons which we can adopt for the facets of particles of large radius (R1), and the second corresponds to squares which we adopt for the facets of particles of small radius (R2).
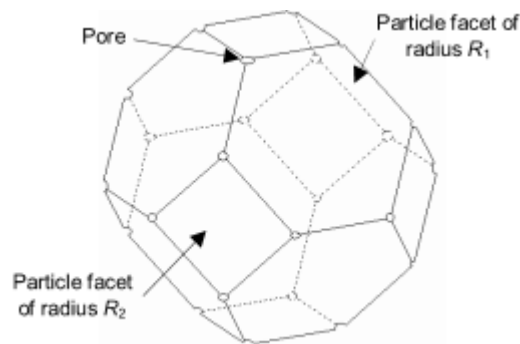

Fig. 2 – Geometric model to describe the two-dimensional particles shape at the final stage of RDP densification.

In this case, we will establish new expressions to evaluate the average contact area between particles and the pore radius at the final stage of densification.

Knowing that a pore is shared between four neighbouring particles, the total area of the contacts can be written as:

$$aZ = 4\pi R^2 - \frac{24}{4}\left(4\pi r_p^2\right) \tag{14}$$

where rp is the spherical pore radius given by:

$$r_{\mathrm{p}} = R \left(\frac{1-D}{6D} \right)^{1/3}$$

(15)

It should be noted that this expression reveals the error existing in the expression established by Arzt et al. [1] and used by several researchers.

As in the final stage Z=14, and after replacing R and rp by their expressions (respectively Eq. 11 and Eq. 15), the average contact area is evaluated by:

$$a = \frac{8}{7} \pi \left(\frac{R_1 R_2}{R_1 + R_2} \right)^2 \left[1 - 6 \left(\frac{1-D}{6D} \right)^{2/3} \right]$$

(16)

2.3 Effective pressure

In the case of constrained sintering, in particular in HIP, another parameter of the RDPs that is very important in the modelling of the densification mechanisms comes into play. It is the effective pressure (P_{eff}) which is the pressure at contact between particles. It depends on the total contact area to the total area of a particle. It is given by [4]:

$$P_{\mathrm{eff}} = \frac{4\pi R^2}{aZ} P$$

(17)

Using this relation, established to study the transmission of stresses through an RDP of spherical particles, we can recalculate P_{eff} equations in the two stages of densification for RDP of two-dimensional spherical particles, replacing Z, a and R by their expressions. The established equations are as follow:

In stage I :

$$P_{\mathrm{eff}} = \frac{16}{Z \left[\left(\frac{D}{D_0} \right)^{1/3} - 1 \right]} \frac{R_1 R_2}{(R_1 + R_2)^2} P$$

(18)

In stage II :

$$P_{\mathrm{eff}} = \frac{1}{\left[1 - 6 \left(\frac{1-D}{6D} \right)^{2/3} \right]} P$$

(19)

3 Results and discussion

3.1 Coordination number

The evolution of the average contacts number per particle as a function of the instantaneous relative density is given in Fig. 3. The curve in solid line (without marker) is obtained using our new approach corresponding to equation (7). To highlight the dissimilarity, we also represented the approaches relating to the RDPs of one-dimensional particles of Arzt [11], Helle [2] and Redouani [5].

The graph indicates that the contacts number per two-dimensional particle increases slowly at the start of densification. At the intermediate step, that is to say when D changes from 0.75 to 0.92, Z increases faster. We can explain this rapid evolution by the morphological transformation generated at the level of the porous phase, it gradually passes from an open and interconnected form to a fine dispersion of spherical pores. Because of this morphological evolution, the coordination number reaches its maximum value (Z=14) when D reaches 92% and remains constant throughout the interval $[0.92 - 1]$.

The shape of the obtained curve of new approach is similar to that obtained by our old approach [5] but with higher values. This seems logical because we have considered particles with different sizes which relatively increase the coordination number.
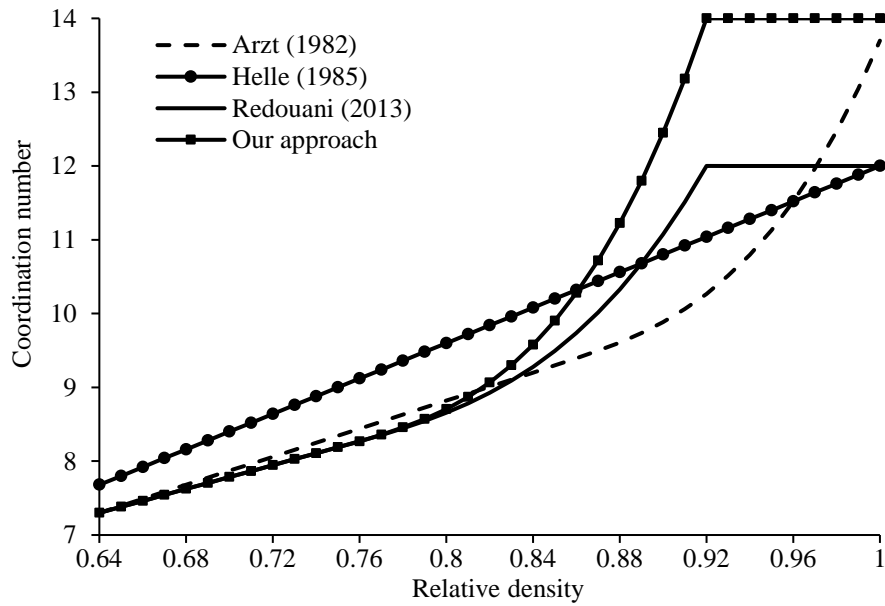
Fig. 3 – Evolution of coordination number as a function of relative density.

3.2 Average contact area

Our approach stipulates that the average contact area as a function of relative density evolves in two stages (stage I and stage II). Using equations (13) and (16), we take as values of the two radii R1 and R2 respectively 10μm and 5μm. The choice of these values is motivated by the fact that it is the average of the micrometric particles size used in general.

The evolution of the contact area for two-dimensional particles is represented by the curve in solid line without marker in Fig. 4. The two other curves represent the evolution of the contact area using the old approach [5] for particles of the same radius with taking the values 10μm and 5μm separately.
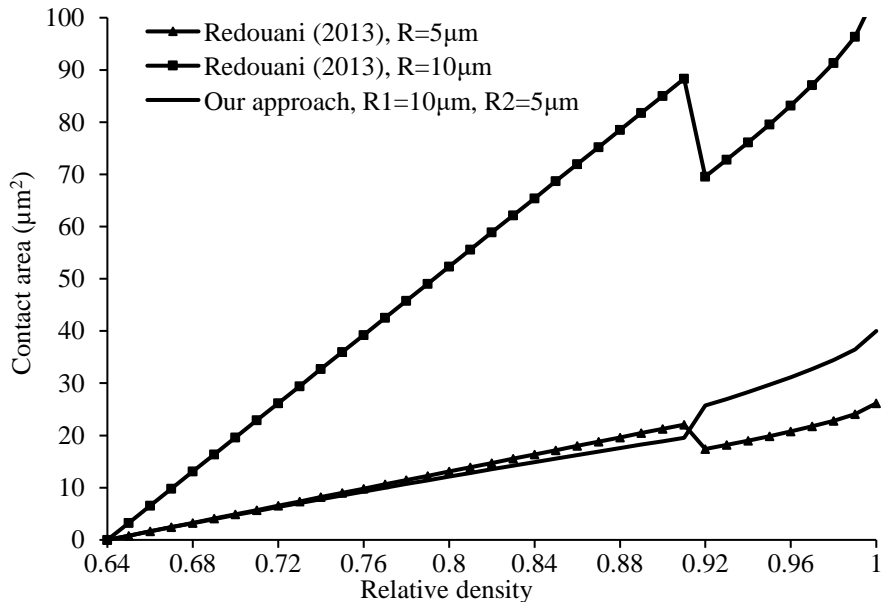

Fig. 4 – Evolution of the average contact area as a function of the relative density.

The curves shown in Fig. 4 give an idea of the evolution of the average contact area as a function of the relative density. For the new approach, we note that in the interval $[0.64 - 0.92]$, the contact area increases linearly and slowly. Then, when

D≥0.92, the area increases rapidly. This change in slope of the curve is due to the change in morphology of the porosity that manifests by the closure and dispersion of the spherical pores.

For the old approach, we observe from the curves of Fig. 4 a questionable discontinuity in the evolution of the contact area at the level of the transition from stage I to stage II. Indeed, this discontinuity corresponds to a decrease in the contact area at the level of this transition, which obviously does not correspond to reality, because actually the contacts between particles increase until the total disappearance of the porosity in the tablets. Unlike our new approach which is more realistic since the discontinuity corresponds rather to an increase and not to the decrease.

To better apprehend the results of our approach, we have drawn several curves for the mean contact area for different values of the radii R1 and R2. From Fig. 5 it can be seen that when R1 and R2 are very different (R1>>R2), the evolution of the contact area decreases when passing from stage I to stage II. This decrease can be explained by the fact that the approximation chosen for the particle radius (Eq. 11) is valid when the two particle sizes are near.
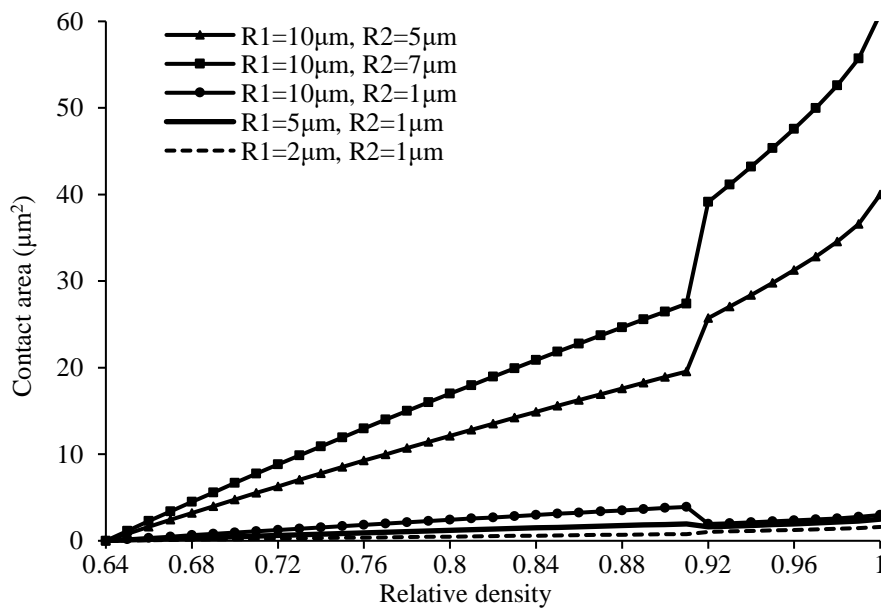

Fig. 5 – Evolution of the average contact area for different values of R1 and R2.

3.3 Effective pressure

The evolution of P_{eff} is represented in Fig. 6 using equations (18) and (19). We have chosen to represent the ratio P_{eff}/P as a function of D in this graph in order to avoid estimating P which has no influence on the shape of the curves. We have also shown in the same figure my old approach [5] for the two radii 10μm and 5μm (separately).

Fig. 6 shows that P_{eff} decreases during densification. At the beginning, the effective pressure tends to infinity because the contact area is punctual. It reaches its minimum value, equal to the applied pressure P, at the end of densification, i.e. when the contact surface is equal to the total area of the powder particle. Indeed, we have seen that the effective pressure depends on the area of a particle compared to the total area. Knowing that in our new approach, we considered that during the densification of the RDPs, the particles areas widen while the total area remains fixed, therefore the pressure exerted at the level of the contacts between particles decreases.

By comparison, the effective pressure calculated using my old approach decreases but with lower values compared to those of the new approach. Also, we note that P_{eff} values are lower when the particle radius is great.

Fig. 7 corresponds to the new approach for different values of the radii R1 and R2. It shows that the shape of the effective pressure curve is not affected by the change in the radii R1 and R2. On the other hand, this change affects the values of the effective pressure, i.e. that the values of P_{eff} are even smaller when the differences between R1 and R2 are greater and the powder particles are smaller. This behaviour is noted in the first stage of densification. In stage II, the values of the effective pressure are the same, between different curves, since this does not depend on the size of the particles but rather on the size of the spherical pores.
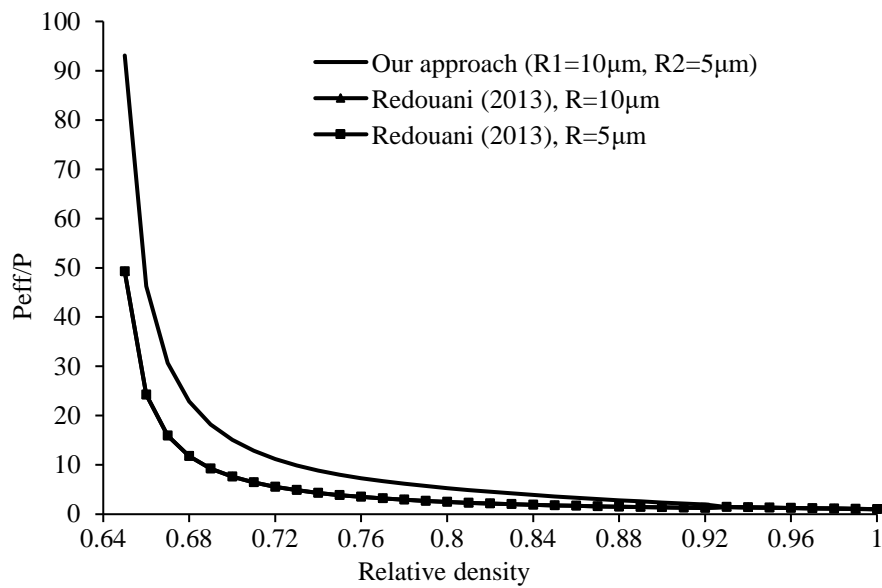
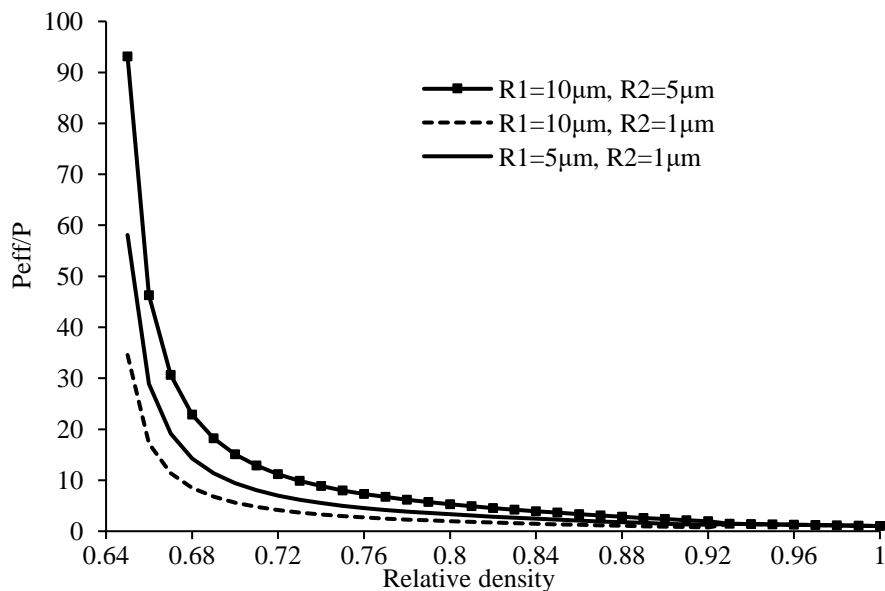**Fig. 6 – Evolution of the effective pressure as function of relative density.**

Fig. 7 – Variation of the effective pressure for different values of R1 and R2.

4   Conclusion

During the HIPing densification, powders can undergo morphological changes. These changes lead to an increase in the number of coordination and a widening of the contact zone until the total density of the system is reached (D=1). The study of densification mechanisms must therefore take into account the evolution of these geometrical parameters. To meet this requirement, we had to assimilate powder aggregates to RDPs of spherical particles of two different sizes. This new approach allowed us to express the coordination number and the mean contact area as a function of the relative density reached in the tablet. The effective pressure was then evaluated using the new Z and a, expressions. The proposed method is used to draw graphs with curves representing the different parameters of the RDPs as a function of the relative density. The figures produced show very good results for relatively close particle radii. Indeed, for the contact zone in particular, our new study has successfully eliminated an inconsistent decrease in the transition from step I to step II. This inconsistency is found in previous approaches to RDPs for spherical particles of the same size. It is clear that further research is needed to better understand the densification process of RDPs. Based on the promising results presented in this paper, work on the remaining questions concerning the study of the densification mechanisms of RDPs is continuing and will be presented in future works.

Acknowledgments

REFERENCES

[1]- E. Arzt, M.F. Ashby, K. Easterling, Practical applications of hot-isostatic pressing diagrams: Four case studies. (1981). 33574. doi:10.1007/BF02651618.

[2]- A.S. Helle, K.E. Easterling, M.F. Ashby, Hot-isostatic pressing diagrams: New developments. Acta Metall., 33(12) (1985) 2163-2174. doi:10.1016/0001-6160(85)90177-4.

[3]- C. Rizkallah, J.P. Fondère, H.F. Raynaud, A. Vignes, Advanced process control of hot isostatic pressing. Application to Astroloy HIP. Revue de Métallurgie, 98(12) (2002) 1109-1128. doi:10.1051/metal:2001151.

[4]- L. Redouani, S. Boudrahem, Hot isostatic pressing process simulation: application to metal powders. Can. J. Phys., 90(6) (2012) 573-583. doi:10.1139/p2012-057.

[5]- L. Redouani. Nouvelle approche de la modélisation de la compression isostatique à chaud de poudres métalliques: utilisation de systèmes modèles et prise en compte des trois étapes du cycle. PhD Thesis. University of Abderrahmane Mira Bejaia, 2013.

[6]- L. Redouani, S. Boudrahem, Simulation of the metal and ceramic powders densification process by hot isostatic pressing. Int. J. Eng. Sci. Innov. Tech., 4(3) (2015) 171-180.

[7]- A.M. Abdelhafeez, K.E.A. Essa, Influences of Powder Compaction Constitutive Models on the Finite Element Simulation of Hot Isostatic Pressing. Procedia CIRP, 55 (2016) 188-193. doi:10.1016/j.procir.2016.07.025.

[8]- C. Van Nguyen, Y. Deng, A. Bezold, C. Broeckmann, A combined model to simulate the powder densification and shape changes during hot isostatic pressing. Comput. Methods Appl. Mech. Eng., 315 (2017) 302-315. doi:10.1016/j.cma.2016.10.033.

[9]- L. Redouani, S. Boudrahem, S. Alem, New hot isostatic pressing (HIP) simulation method with taking into account of the operating cycle ramp. Int. J. Adv. Manuf. Tech. 102(9)(2019) 3291-3299. doi:10.1007/s00170-019-03395-w.

[10]- A. Basyir, A.S. Wismogroho, D. Aryanto, W.B. Widayatno, Effect of hot isostatic pressing method to enhance quality of tin powder. AIP Conf. Proc., 2256(1) (2020) 030021. doi:10.1063/5.0014653.

[11]- E. Arzt, The influence of an increasing particle coordination on the densification of spherical powders. Acta Metall., 30(10) (1982) 1883-1890. doi:10.1016/0001-6160(82)90028-1.

[12]- V. Guerin. Prédiction et compréhension de la densification des poudres commerciales d'alumine et de fer grâce à une approche par réseau de neurones artificiels. (2004).

[13]- L. Olmos, T. Takahashi, D. Bouvard, C.L. Martin, L. Salvo, D. Bellet, M. Di Michiel, Analysing the sintering of heterogeneous powder structures by in situ microtomography. Philos. Mag., 89(32) (2009) 2949-2965. doi:10.1080/14786430903150225.

[14]- B. Jasper, J.W. Coenen, J. Riesch, T. Höschen, M. Bram, C. Linsmeier, Powder Metallurgical Tungsten Fiber-Reinforced Tungsten. Mater. Sci. Forum, 825-826 (2015) 125-133. doi:10.4028/www.scientific.net/MSF.825-826.125.

[15]- G. Roquier, A Theoretical Packing Density Model (TPDM) for ordered and disordered packings. Powder Technol., 344 (2019) 343-362. doi:10.1016/j.powtec.2018.12.033.

[16]- Y. Feng, B. Gong, H. Cheng, L. Wang, X. Wang, Effects of fixed wall and pebble size ratio on packing properties and contact force distribution in binary-sized pebble mixed beds at the maximum packing efficiency state. Powder Technol., 390 (2021) 504-520. doi:10.1016/j.powtec.2021.05.099.

[17]- H.N.G. Wadley, T.S. Davison, J.M. Kunze, Densification of metal coated fibers by elastic-plastic contact deformation. Composites Part B, 28(3) (1997) 233-242. doi:10.1016/S1359-8368(96)00044-3.

[18]- [18]- S.M. Sweeney, C.L. Martin, Pore size distributions calculated from 3-D images of DEM-simulated powder compacts. Acta Mater., 51(12) (2003) 3635-3649. doi:10.1016/S1359-6454(03)00183-6.

[19]- C. Martin, D. Bouvard, S. Shima, Study of particle rearrangement during powder compaction by the discrete element method. J. Mech. Phys. Solids, 51(4) (2003) 667-693.

[20]- F.B. Swinkels, D.S. Wilkinson, E. Arzt, M.F. Ashby, Mechanisms of hot-isostatic pressing. Acta Metall., 31(11) (1983) 1829-1840. doi:10.1016/0001-6160(83)90129-3.